MODELING OF TRITIUM BEHAVIOR IN SOLID BREEDERS

by
A.R. Raffray
M.A Abdou
Mechanical, Aerospace and Nuclear Engineering Department
6288 Boelter Hall
University of California at Los Angeles
Los Angeles, CA 90024

P.J. Gierszewski
Canadian Center for Fusion Fuels Technology
2700 Lakeshore Road West
Mississauga, Ontario Canada L5J 1K3

Symposium on "Fabrication and Properties of Lithium Ceramics"
American Ceramic Society
Pittsburg
April 26-30, 1987

Work supported under Department of Energy Grant No. DE-FG03-86ER52123

I. INTRODUCTION

Modeling of the steady and unsteady tritium behavior in solid breeders complements tritium experiments since it helps in the interpretation of experimental data and in the determination of tritium-related properties of solid breeders. In addition, a model which couples the different tritium transport mechanisms provides the possibility of observing their specific contributions to the overall tritium behavior and could be used an important element in the total tritium cycle modeling. Finally, a model with transient capabilities would provide information on the cyclic behavior of tritium transport and could define useful operating conditions for an engineering test reactor. This paper describes a computer model, MODELT, which is being developed for the above purposes and discusses its initial results.

II. TRITIUM TRANSPORT MECHANISMS

Figure 1 shows the five tritium transport mechanisms which are modeled. The tritium produced in the solid breeder grain diffuses in atomic form in the grain and grain boundary, and then desorbs in the pores as molecules in combination with any oxygen or hydrogen present. Tritium then diffuses in the pores to the purge flow, where it is convected outside the solid breeder.

The model assumes that porosity is interconnected from the grain boundary to the purge flow and considers as a unit cell one interconnected porosity system, including the surrounding breeder grains. The equations used for the different transport mechanisms are shown below. Tritium solubility in the solid breeder would affect the intragranular diffusion equation, but it is not considered here for simplicity.

Intragranular Diffusion

The solid breeder grains are assumed to be spherical and the equation of continuity is:

$$D_g(T)\left(\frac{1}{r^2}\frac{\partial}{\partial r}(r2\frac{\partial C_g}{\partial r})\right)+\dot{G}(t)=\frac{\partial C_g}{\partial t} \qquad (1)$$

where D_g is the tritium diffusion coefficient in the solid breeder, T is the temperature, C_g is the tritium concentration per unit volume, and G_g is the generation rate per unit volume.

The boundary conditions are symmetry at the grain center and continuity of concentration at the grain and grain boundary interface.

$$\frac{\partial C_g}{\partial r} = 0 \qquad \text{at } r = 0 \tag{2}$$

$$C_g = C_{gb} \qquad \text{at } r = r_g \tag{3}$$

where C_gb is the tritium concentration in the grain boundary and r_g is the solid breeder grain radius.

Grain Boundary Diffusion

Diffusion is assumed to be one-dimensional and the equation of continuity is:

$$D_{gb}(T)\frac{\partial^2 C_{gb}}{\partial x^2} = \frac{\partial C_{gb}}{\partial t} \tag{4}$$

where D_{gb} is the tritium diffusion coefficient in the grain boundary and x is the distance along the grain boundary.

The boundary condition is determined by the effective desorption mass transfer coefficient, h_m:

$$-D_{gb}\frac{\partial C_{gb}}{\partial x} = h_m C_{gb} \qquad \text{at } x = x_{gb} \tag{5}$$

where x_{gb} is the length of the grain boundary diffusion path.

Grain boundary diffusion is assumed to be much faster than intragranular diffusion and is not expected to affect the results shown here. It is included in the model, however, for future calculations.

Adsorption and Desorption

From Ref. [1], for hydrogen adsorption on oxides, physisorption predominates at low temperatures and chemisorption at higher temperatures. Two modes of chemisorption have been observed: a rapid, weak and reversible chemisorption at moderate temperatures

and a slower, stronger and irreversible chemisorption at the higher temperatures of interest here. Hydrogen gas adsorption then occurs with dissociation and desorption only occurs as water, suggesting the following mechanism [1]:

$$\text{Desorption} \quad 2\,OH^- \rightarrow 0^{2-} + H_20 \tag{6}$$

$$\text{Adsorption} \quad \frac{1}{2}H_2 + 0^{2-} \rightarrow OH^- + e \tag{7}$$

Assuming that water adsorbs with the formation of the hydroxyl group [2], this suggests that experimental data for water desorption could be used to estimate hydrogen desorption. It should be noted that in solid breeder experiments such as TRIO [3], the released tritium form was mainly HT. This is not necessarily in contradiction with Eq. (6), however, as reduction through the purge lines could have occurred. Accurate data on the form of desorbed tritium from solid breeders from controlled adsorption/desorption experiments would be very useful. For activated adsorption, the rate of adsorption, u (molecules/m^2 - s), may be formulated in terms of the adsorption activation energy, E, and probability factors [1].

$$u = \frac{\sigma P}{(2\pi mkT)^{1/2}} f(\theta)\, e^{-E/RT} \tag{8}$$

where:

σ = condensation coefficient (probability that a molecule, with the required energy, colliding with a vacant site will get adsorbed)

θ = coverage = (number of occupied sites/total number of sites)

$f(\theta)$ = probability that a collision will take place at an available site $\cong (1 - \theta)^2$ for adsorption with dissociation

$\frac{P}{(2\pi mkT)^{1/2}}$ = number of colliding molecules per unit surface area per unit time

P = pressure

m = mass of molecule

k = Boltzmann constant

R = universal gas constant

For activated desorption, the rate of desorption, u' (molecules/m^2-s), can be expressed in terms of the desorption activation energy, E', and probability factors [1]:

$$u' = K_d\, f'(\theta)\, e^{-E'/RT} \tag{9}$$

where:

K_d = velocity constant $\cong \frac{n_S\, kT}{h}$ for desorption with association from statistical mechanics and partition function consideration

n_S = total number of sites per unit area of surface

h = Planck's constant

$f'(\theta)$ = fraction of sites available for desorption $\cong \theta^2$ for desorption with association

E' = activation energy for desorption

Pore Diffusion

The interconnected porosity is modeled as a cylinder and the equation of continuity is used for each gas species (i = H_2, T_2 and HT):

$$\varepsilon\, D_{p_i}(T) \frac{\partial^2 C_{p_i}}{\partial z^2} + \dot{G}_{p_i} = \frac{\partial C_{p_i}}{\partial t} \tag{10}$$

where the porosity, ε, is used as a correction term for the diffusion coefficient, D_{p_i}, to account for pore tortuosity. C_{p_i} is the concentration of the gas species per unit volume of the interconnected porosity and $\dot{G}_{p_i}$ is the source term corresponding to the amount of desorbed and adsorbed gas species along the pore.

III. GEOMETRY

For a given porosity, ε, and grain radius, r_g, the sperical pore radius, r_{pore}, is calculated from the following expression [4]:

$$r_{pore} = 0.406\, r_g \left(\frac{\varepsilon}{1 - \varepsilon}\right)^{1/2} \tag{11}$$

Since the interconnected porosity is assumed to have a cylindrical geometry, each pore is also assumed to be cylindrical, of length ($2\,r_{pore}$) and of radius, r_p. For the same pore volume, V_p, r_p can be calculated as follows:

$$r_p = \left(\frac{2}{3}\right)^{1/2} r_{pore} \tag{12}$$

The number of grains per interconnected porosity system can be determined from the grain and pore sizes, the porosity and the length of the interconnected porosity system. The grains are considered as forming an annular cluster around the interconnected pores as shown in Fig. 1. The outer radius of this cluster, r_{clus}, is evaluated from r_{pore}, V_p and ε.

$$r_{clus} = \left(\frac{V_p}{\pi\,\varepsilon\,r_{pore}}\right) \tag{13}$$

The length of the interconnected porosity system to the convective purge flow region is dependent on the solid breeder geometry. For sphere-pac form, for example, the length would be approximately equivalent to the radius of a solid breeder sphere.

Grain boundary diffusion is assumed to be much faster than intragranular diffusion and is not expected to affect the initial results described here. For that reason the choice of the geometry for the grain boundary diffusion is not discussed.

IV. PROPERTY DATA AND PARAMETERS

Initial results were obtained for $LiAlO_2$ with parameters corresponding to the TRIO experiment [3] and listed in Table 1. The following property data was used.

Intragranular Diffusion [1]

$$D_g\ (m^2/s) = 1.1 \times 10^{-10} \exp\,[-0.135\ (MJ/mol)\ /RT] \tag{14}$$

Note that there is an uncertainty factor of about 5 in D_g.

Grain Boundary Diffusion

For present purposes, D_{gb} was set arbitrarily as ($10^5\ D_g$), assuming that grain boundary diffusion is much faster than intragranular diffusion.

Pore Diffusion [6]

$$D_{pi}\,(m^2/s) = \frac{0.04356\ T^{1.5}}{P(V_a^{1/3} + V_b^{1/3})^2}\left(\frac{1}{M_a} + \frac{1}{M_b}\right)^{1/2} \qquad (15)$$

where:

P and T are in Pa and K, respectively

M_a and M_b = molecular weights of the two gases

V_a and V_b = atomic volumes

= 14.3 for hydrogen (15.0 was assumed for helium)

Desorption Mass Transfer Coefficient [7]

$$h_m\,(m/s) = 6.45\ \exp[-0.1285\ (MJ/mol)\ /RT] \qquad (16)$$

Desorption and Adsorption Activation Energies

Experimental data on water desorption Al_2O_3 (from Morimoto, et al., [2]) was used to estimate the desorption activation energy as a function of coverage for hydrogen. For that experiment, a heat treated Al_2O_3 sample was exposed to saturated water vapor. The sample was then degassed for four hours in a vacuum of 10^{-5} Torr at a given temperature. The degassing was repeated for progressively increasing evaporation temperatures. Since the amount of water expelled was negligible at the highest temperature, it was assumed that the amount of adsorbed water at 1100°C was zero for calculation purposes.

Table 2 shows the results from Ref. [2] and their interpretation to obtain the desorption activation energy as a function of coverage by using Eq. (9). N_h is the amount of adsorbed OH group at each temperature and the coverage, θ, is calculated using the area of the hydroxyl group as 5 Å^2 (with a corresponding number of 20 OH groups/100 Å^2 for full coverage, $\theta = 1$). The difference between successive values of N_h, ΔN_h, is assumed to represent the number of hydroxyl groups which desorbed at the given temperature and coverage over the four hours.

The results are illustrated in Fig. 2, which shows the variation of desorption activation energy with coverage. Note, however, that the values of E' at the higher coverages are not as accurate since they were obtained at lower temperatures where a different mode of chemisorption or even physisorption could occur appreciably. Curve fitting the data yields the following expression:

$$E'(MJ/mol) = 0.108 - 0.0645 \ln \theta \qquad (17)$$

The desorption activation energy falls with increasing coverage. Possible explanations for this are based on the discussion in Ref. [1]. The first is that for a heterogeneous surface, the most active sites are covered first by adsorption and as the coverage increases sites of lessening activity are then covered. At high coverage, desorption occurs first from the sites of lesser activity, and the activation energy for adsorption decreases with coverage. The other possible explanation is that this is due to the forces of repulsion between molecules in the adsorbed layer. These forces increase with coverage and encourage desorption, whose activation energy decreases.

The same type of argument indicates that the activation energy for adsorption, E, increases with coverage. However, since no data were found for E as a function of θ, a constant E was assumed for each set of calculations.

Substituting Eq. (17) in Eq. (9) for E' and replacing u' by $\left(-ns\ \frac{\partial\theta}{\partial t}\right)$ yields an expression which can be integrated to obtain time, t, as a function of coverage, θ. The initial condition is that θ is assumed to be 1 (i.e. full coverage) at time o. The results are shown in Fig. 3. At coverages between 0.1 and 0.2, the time to desorb is large at the lower temperature (700 K), of the order of 10^4 - 10^6 s. However, at the higher temperatures (973 K and 1100 K), desorption is much faster (with desorption times of 0.01 to 1 s for coverages between 0.1 and 0.2).

V. SOLUTION METHOD

At each time step, the intragranular and grain boundary diffusion equations (Eqs. 1 and 4) are solved simultaneously using an implicit finite difference formulation and the boundary equations shown in Eqs. (2), (3), and (5).

To facilitate the calculation procedure, the solution of the grain and grain boundary diffusion equations is separated from the solution of the pore diffusion and surface adsorption and desorption equations. In particular, the desorption mass transfer of the diffusing tritium atoms from the grain boundary to the pore is assumed to only occur as tritium molecules and to be proportional to the tritium atom concentration in the grain boundary (see Eq. 5). This is based on the assumption that a diffusing tritium atom has a probability proportional to the concentration of the tritium atoms of finding another tritium atom before desorbing. However, once the tritium molecule gets into the pore, its contributions to the partial pressure of the gas species and, hence, to the adsorption according to Eq. (8), and to

the subsequent desorption according to Eq. (9) are considered. Note that the probability of two adsorbed components at two different sites to associate and desorb is now proportional to the square of the coverage (as shown in Eq. (9)).

From a global point of view, once the diffusing tritium atom desorbs as tritium molecules, they are involved in the complete adsorption and desorption processes. For that reason, although the above assumption is physically incorrect since a diffusing tritium atom could associate with an adsorbed component and desorb, the effect of this assumption on the results is believed to be small.

For adsorption and desorption, the steady state coverage at the start of the transient process is first calculated by equating Eqs. (8) and (9). The transient calculation then proceeds by evaluating the number of desorbed and adsorbed molecules. Only the three gas species, H_2, T_2 and HT are considered in the calculation under the asssumption that all H_2O, T_2O and HTO are reduced. The concentrations of the gas species in the pores are first calculated using the mass transfer from the grain boundary as the only source term. The initial value of the coverage, θ_{n+1}, at the end of the time step, Δt, is obtained by equating Eqs. (8) and (9). The total number of desorbed molecules per unit area, N_d, is then calculated over the time step as follows (with $\Delta\theta = \theta_{n+1} - \theta_n$)

$$N_d = \frac{\Delta t}{\Delta\theta} \int_{\theta}^{\theta+\Delta\theta} u' \, d\theta \tag{18}$$

Before carrying the integration, Eq. (17) which gives E' as a function of θ, is substituted in the equation for the rate of desorption, u' (Eq. (9)).

The total number of adsorbed molecules per unit area, N_a, is obtained from the number of desorbed molecules per unit area, N_d, the number of sites per unit area, n_S, and the change in coverage, $\Delta\theta$.

$$N_a = N_d + 0.5 \, n_S \, \Delta\theta \tag{19}$$

For each gas species, the following constraints on N_a and N_d are imposed at each time step corresponding to the maximum possible mass flux in the pore and to the available number of adsorbed molecules respectively. These constraints are conservative since only the molecules available for adsorption and desorption prior to the time step are considered.

Adsorption: $$N_a < f_a \, D_{p_i} \, C_{p_i} \, A \, a_p \, \Delta t/(\Delta z_p \, a_a \, M_i) \tag{20}$$

Desorption: $$N_d < 0.5 \, f_d \, \theta_i \, n_s \tag{21}$$

(note that the 0.5 factor is to account for desorption with association)

Where:

f_a, f_d = control factors (assumed to be 0.5 for the initial calculations)

Δt = time step

Δz_p = spatial increment in pore

θ_i = species coverage

M_i = species molecular weight

a_a = adsorption area

a_p = pore diffusion area

A = Avogadro's number

The new value for the coverage at the end of the time step, θ_{n+1}, is then calculated from:

$$(\theta_{n+1})_{new} = \theta_n + (N_a - N_d)/(0.5\ n_S) \qquad (22)$$

where the factor of 0.5 accounts for the fact that a molecule dissociates and occupies two sites when adsorbing. An iterative process is required using Eqs. (18) and (19) to calculate N_d and N_a from θ_{n+1} subject to Eqs. (20) and (21) constraints,and using Eq. (22) to then calculate new values for θ_{n+1} from N_a and N_d until the difference between the old and new values of θ_{n+1} is acceptable.

Note that the reason to base the iterative calculation process on determining N_d from the equation for u' (and not N_a from the equation for u), is that the only data available were for the desorption activation energy as a function of coverage. Thus, the adsorption activation energy is assumed constant and affects the results only be setting the initial steady state cover age prior to the transient calculation. The total number of adsorbed molecules is divided between the three gas species according to the fraction contributed by each species to the effective ($\Sigma\ P_i/\sqrt{m_i}$) term. Similarly, the total number of desorbed molecules are divided between the three species according to their individual coverage at each time step.

The gas species desorption/adsorption calculations are performed at each spatial zone in the interconnected porosity. The pore diffusion equation (Eq.10) is then solved for each gas using the grain boundary mass transfer and the desorption or adsorption mass

flux as source terms. After each computation of the gas concentrations, the concentrations are corrected from the following equation assuming isotope exchange is very fast.

$$\frac{P_{HT}^{2}}{P_{T_2} \cdot P_{H_2}} = k_{eq} \tag{24}$$

(For these initial calculations, k_{eq} is assumed to be equal to 1)

VII RESULTS

The initial results discussed here were directed principally toward observing the effect of increasing the hydrogen fraction in the purge flow on the transient tritium release.

Figure 4 shows the steady state coverage as a function of adsorption activation energy for different H_2 volumetric fractions in the sweep gas (or purge flow). For the 0.0001% H_2 case, most of the coverage is due to the tritium in the pore, while for the higher H_2 volume fractions most of the coverage is due to H_2. At the lower values of E, the difference in θ between the various cases is quite large.

Note that the constraints on N_a and N_d (Eqs. 21 and 22) would cause a delay before the coverage could reach steady state after a transient change in the H_2 volume fraction in the purge flow. Hence, for the results discussed below the coverages over the time periods shown only change incrementally and are still far from the steady state values.

Figure 5 shows the transient tritium released from the end of the interconnected porosity system with tritium generation starting at time zero. Four cases are shown: one with no adsorption/desorption taking place (i.e. essentially a diffusive process) and the three others with adsorption/desorption taking place with an adsorption activation energy of 0.18 MJ/mol, but with different volume fractions of H_2 in the purge flow. For the case with no adsorption/desorption, the results correctly show the diffusion-controlled characteristics of the tritium released (normalised to the tritium generated) approaching the steady state value of 1.0. The other cases demonstrate the advantage of having an amount of H_2 in the purge flow which swamps the amount of T_2 released. Then, tritium adsorption scarcely occurs and the diffusive processes dictate the shape of the curve. However, with very small amount of H_2 in the purge flow (0.0001% H_2), tritium adsorption is significant and it takes over 150 s in this case for any tritium to be released from the interconnected porosity and the time to reach steady state is appreciably increased.

Figure 6 shows the results obtained from parameters corresponding to the TRIO Run 3 [3]. At time = 0 s, the H_2 volume fraction in the purge flow is changed from 0.1%

to 1%. The time for hydrogen to diffuse through the interconnected porosity to the breeder surface is relatively short and the surface coverage increases with the increased hydrogen partial pressure. The adsorbed tritium is basically replaced by the hydrogen and a surge in the tritium released can be observed with peaks depending on the adsorption activation energy (i.e. on the initial coverage). The peak from the TRIO experiment is about 1.7, but only occurs after a time lag of about 0.5-1 hour and also occurs over a time period of about 0.5-1 hour also.

Thus, although it is encouraging that the shape of the TRIO tritium release curve is reproduced in Fig. 6, the time scale is different by about two orders of magnitude. This difference in time scales could be due to the following factors relating to the model. The modeling is still at an early stage and there could be phenomena not included in the model (such as solubility) which would affect the tritium release results. The simplification of the geometries whereby the grain, grain boundary and pore are considered as a sphere, slab and cylinder could also affect the modeling results. In addition, some of the property data used have uncertainties associated with them. In particular, experimental data are needed that can be used to estimate more accurately the hydrogen and/or tritium diffusion coefficient in the solid breeder and the hydrogen and/or tritium activation energy for adsorption and desorption as a function of coverage. On the experimental side, adsorption in the lines and the time response of the tritium measuring apparatus could affect the lag time. All these effects need to be further investigated.

Figure 7 shows the tritium released as a function of time for different increases in the H_2 volume fraction to a final value of 0.1%. The peak tritium release decreases markedly as the initial H_2 volume fraction changes from 0% to 0.01%. Figure 8 shows the tritium release over time for several values of the adsorption activation energy for a change in H_2 volume fraction from 0.0001% to 0.1% at time = 0 s.

Comparison of the results from Fig. 8 to those of Fig. 6 shows that for the same adsorption activation energy, the peak tritium release for the former case is higher by close to one order of magnitude than that of the latter case. This is also in accordance with the TRIO results for Runs 3 and 15 (which has the H_2 volume fraction changing from 0% to 0.1%) [3]. The peak tritium released for Run 15 is at least 19. However, the experimental time scale is different from the one obtained from the model. The peak occurs over a time period of about 0.5-1 hour which is again higher than the computed one by about two orders of magnitude.

By equating the peak tritium released for the two cases considered to that of the corresponding TRIO Runs 3 and 15, adsorption activation energies of about 0.23 MJ/mol and 0.21 MJ/mol are obtained, respectively. These would provide a lower limit for E'

since adsorption is exothermic and the heat of adsorption (E' - E) must be positive. In that case, from Fig. 2, the coverage is restricted to values less than about 0.2 for the calculations to be valid.

From Fig. 2, it seems that E should be closer to 0.1 MJ/mol particularly if it increases with θ and if (E' - E) must be positive. This again indicates the need for adsorption and desorption data for hydrogen or tritium which could be used to calculate the adsorption and desorption activation energies as a function of coverage.

Figure 9 shows the effect of a change in the pore diffusion coefficient on the transient tritium release for the case where the H_2 volume fraction changes from 0.0001% to 0.1% at time = 0 s. The effect is quite marked when the pore diffusion coefficient is reduced by a factor of 10. Then, not only does the increased hydrogen diffuse slower through the pore, but the constraint on the maximum possible adsorption mass flux (Eq. (20)) is also stiffer. The result is about a 700% reduction in the tritium release peak. The inverse effects occur when the pore diffusion coefficient is increased by a factor of 10 but the tritium release peak increases only by 70%.

VII. SUMMARY

A model for predicting the steady state and transient tritium behavior in solid breeders is being developed. The model includes grain and grain boundary diffusion of the tritium atom, adsorption/desorption of molecules and the diffusion of different gas species (H_2, T_2, HT) in the pores. The model has been used for parametric studies with emphasis on the time-dependent response. The following observations can be made regarding the model based on the literature and on the initial results.

At higher temperatures, for hydrogen adsorption on oxides (such as Cr_2O_3 and $ZnO \cdot Cr_2O_3$ [1]), activated chemisorption with dissociation is believed to predominate. The chemisorption is irreversible with desorption occuring as water.

From past experimental results [2], the activation energy of desorption of hydroxyl groups from Al_2O_3 has been estimated as a function of coverage. The calculated desorption activation energy decreases with coverage. Based on these results, the estimated time needed for the surface hydroxyl groups to desorb from Al_2O_3 increases rapidly with decreasing coverage and/or temperature. At high temperature (1100 K) for coverages greater than 0.05, the time to desorb is less than about 10 seconds. However, at low temperature (700 K), for coverages greater than 0.1, the time to desorb is at least 10^6 seconds.

It seems possible to model transient activated adsorption and desorption by using expressions for the desorption and adsorption rates based on the respective activation ener-

gy and probability factors. For each step in the numerical solution, these desorption and adsorption rates are constrained by the available number of adsorbed molecules and the diffusive mass flux in the interconnected porosity, respectively.

Based on the model results, the hydrogen volume fraction in the purge flow was found to have an appreciable effect on the transient tritium release for a step change in the tritium generation. Cases with hydrogen volume fractions higher than about 1% cause the adsorption surface to be virtually saturated with hydrogen and little tritium is adsorbed. The tritium release then is essentially controlled by diffusion. Cases with lower hydrogen volume fractions (0.0001%) result in considerable tritium adsorption, a lag time before any tritium is released and a delay in the attainment of steady state.

Two cases were modeled with a step increase in the hydrogen volume fraction in the purge flow (based on TRIO parameters). They show an initial tritium-release peak over a period of 10 to 100 seconds. The size of the peak increases with decreasing values of the adsorption activation energy and/or increasing values of the pore diffusion coefficient.

The time scale for the TRIO experiment is about two orders of magnitude higher than obtained here. However, the modeling is still at an early stage and there are phenomena not included in the model (such as solubility) which could affect the tritium release results. The simplification of the geometry where by the grain, grain boundary and pore are considered as a sphere, slab and cylinder could also affect the results. In addition, some of the property data used have uncertainties associated with them. For these reasons, the model and the data base need to be further developed. In particular, experimental data are needed that can be used to estimate more accurately the hydrogen and/or tritium diffusion coefficient in the solid breeder and the desorption and adsorption activation energies as a function of coverage.

Some of the issues that need to be addressed in the future to improve the model include: a) determination of the effect of the geometric assumptions and property data uncertainties on the results; b) determination of the effect of adsorption in the lines on the time scale of tritium release; c) more accurate modeling of grain boundary diffusion and determination of its effect on tritium transport; d) inclusion of solubility in the calculations; and e) inclusion of other species such as H_2O, HTO, T_2O and O_2 in the pore diffusion calculation.

References

1. D.O. Hayward and B.M.W. Trapnell, Chemisortion, second edition, Butterworth, London, 1964

2. T. Morimoto, M. Nagao and J. Imai, "The Adsorption of Water on SiO2, Al_2O_3, and $SiO_2Al_2O_3$. The Relation between the Amount of Physisorbed and Chemisorbed Water,"Bulletin of the Chemical Society of Japan, 44, 1282-1288 (1971)

3. R. Clemmer, et al., "The TRIO Experiment," ANL-84-55, Argonne National Laboratory (1984)

4. C.E. Kessel, "Tritium Behavior in Fusion Reactors", M.S. Thesis, University of California, Los Angeles (1984)

5. M.A. Abdou, M.S. Tillack, A.R. Raffray, A.H. Hadid, et al., "Modeling, Analysis and Experiments for Fusion Nuclear Technology (FNT Progress Report: Modeling & FINESSE)," PPG-1021, UCLA-ENG-86-44, FNT-17, University of California, Los Angeles (January 1987)

6. W.M. Rohsenow and H.Y. Choi,Heat, Mass and Momentum Transfer, Prentice-Hall, Inc., New Jersey (1961)

7. P.C. Bertone, "The Kinetics that Govern the Release of Tritium from Neutron Irradiated Lithium Oxide," Ph.D. Dissertation, Princeton University, June 1980

8. M.C. Billone, "The Influence of Surface Desorption on Tritium Recovery and Inventory in Fusion Solid Breeders,"Journal of Nuclear Materials, 141-143, 316-320 (1986)

Table 1. List Of Parameters Corresponding
To The Trio Experiment [3]

Solid Breeder	
Material	$LiAlO_2$
Density	2.6 g/cm^3
Grain radius, r_g	0.1 μm
Interconnected porosity path length	1.0 mm
Tritium generation rate, $\dot{G}_g$	3.74×10^{-4} g/m^3 - s
Purge Flow	
Gas	Helium
Pressure	3.4×10^5 Pa
Adsorption/Desorption	
Number of sites per unit area, n_S [1,8]	$1 \times 10^{19}/m^2$
Adsorption area [8]	0.45 m^2/g
Condensation coefficient, σ [1]	0.4

Table 2 Desorption Activation Energy, E', for Surface Hydroxyl Groups on Al_2O_3 Calculated from Experimental Data of Morimoto, et al [2]

T(°C)	N_h (OH/100 Å^2)	θ (N_h/20)	Desorption, ΔN_h (OH/100 Å^2)	E' (MJ/mol)
100	11.92	0.596	3.64	0.125
200	8.28	0.414	2.24	0.150
300	6.04	0.302	1.46	0.192
400	4.58	0.229	1.78	0.222
500	2.80	0.140	1.20	0.253
600	1.60	0.080	0.82	0.282
700	0.78	0.039	0.29	0.314
800	0.49	0.025	0.49	0.331
1100	0.0		0.0	

FIGURE CAPTIONS

Figure 1 Mechanisms of tritium transport in solid breeders

Figure 2 Activation energy for H_2O desorption from Al_2O_3 as a function of coverage based on data of Morimoto, et al. [2]

Figure 3 Estimated time for H_2O desorption from Al_2O_3 as a function of coverage and temperature

Figure 4 Calculated steady state coverage as a function of adsorption activation energy for different H_2 volume fractions in the purge flow

Figure 5 Calculated tritium released over time for no adsorption/desorption and for adsorption/desorption with different H_2 volume fractions in the purge flow

Figure 6 Calculated tritium released over time for different constant adsorption activation energies

Figure 7 Calculated tritium released over time for different H_2 volume fraction changes at time zero

Figure 8 Calculated tritium released over time for different constant adsorption activation energies

Figure 9 Calculated tritium released over time for different pore diffusion coefficients

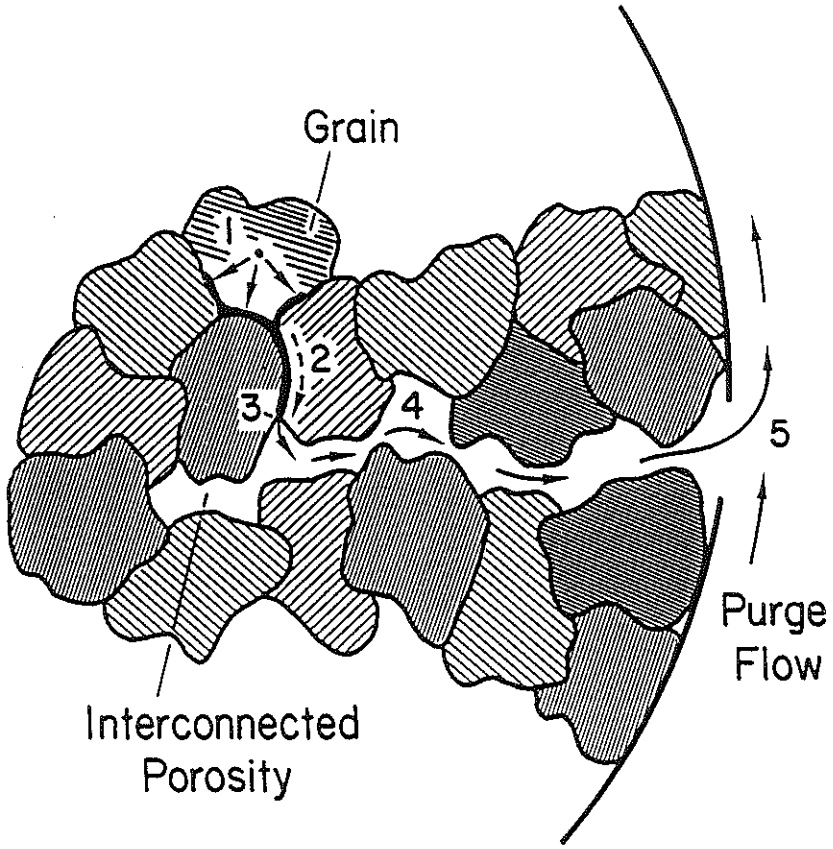

1) Intragranular Diffusion
2) Grain Boundary Diffusion
3) Surface Adsorption / Desorption
4) Pore Diffusion
5) Purge Flow Convection

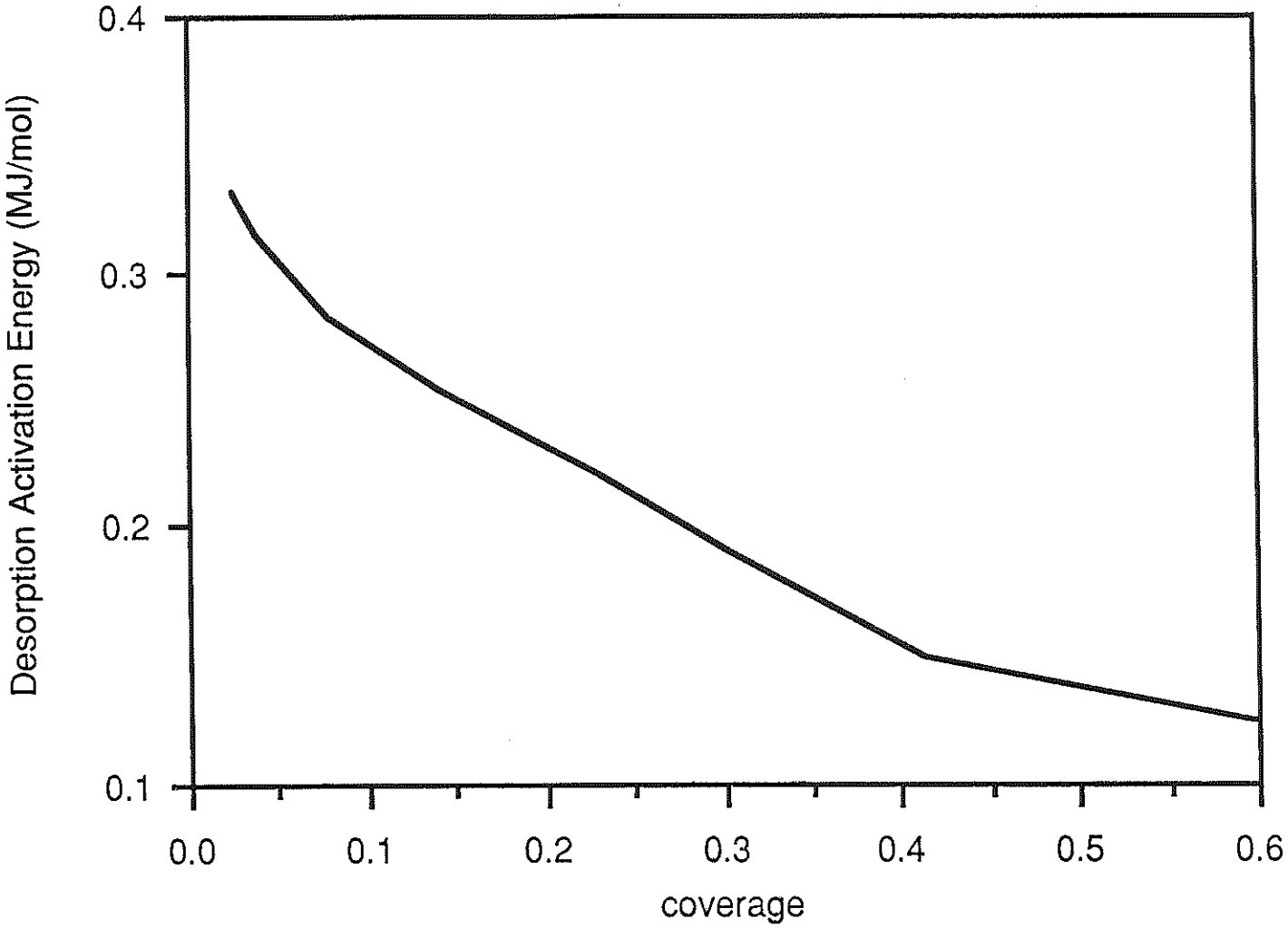
Desorption Activation Energy (MJ/mol)
0.4
0.3
0.2
0.1
0.0
0.1
0.2
0.3
0.4
0.5
0.6
coverage

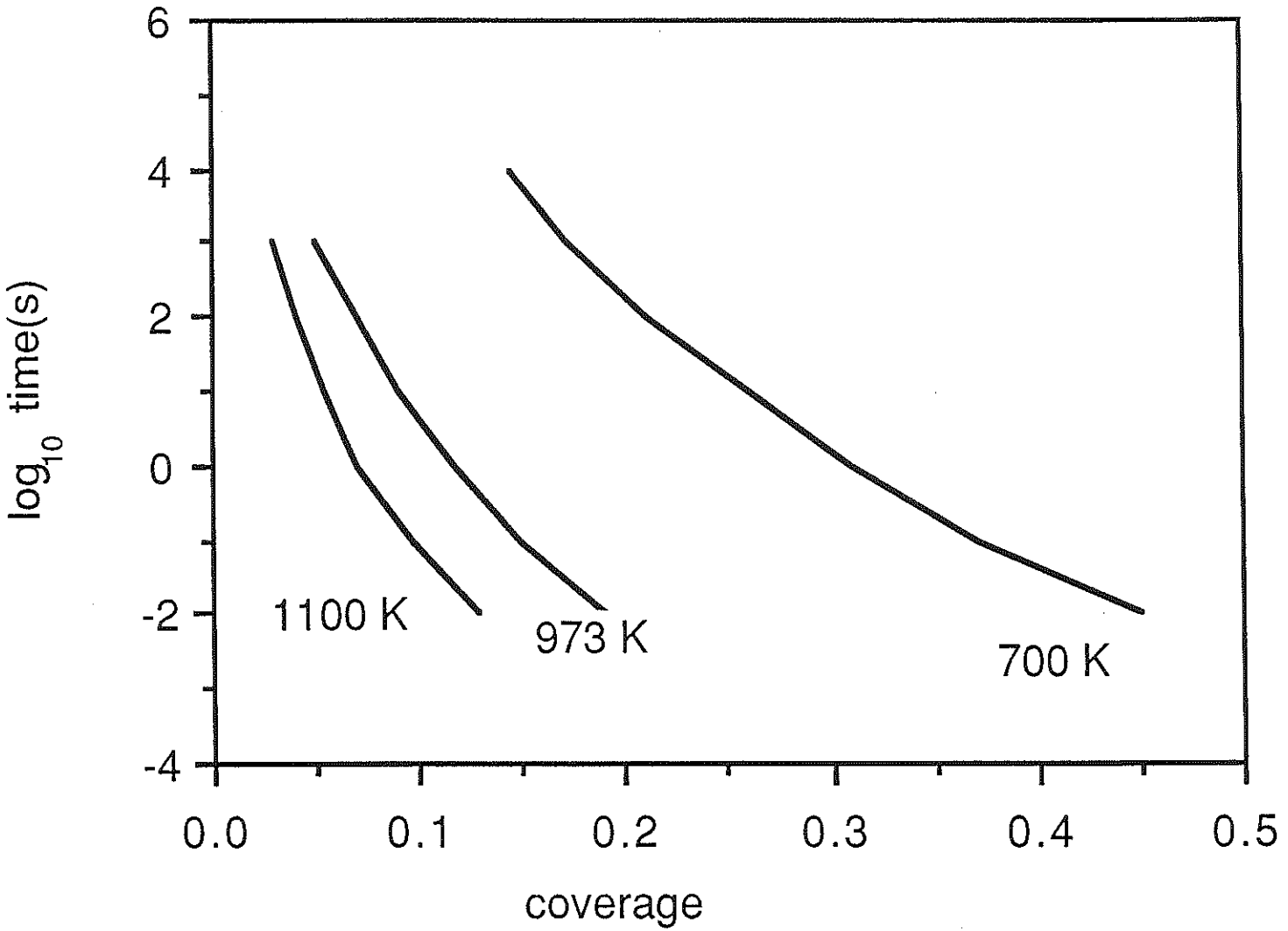
6
4
2
0
-2
-4
log10 time(s)
1100 K
973 K
700 K
0.0
0.1
0.2
0.3
0.4
0.5
coverage

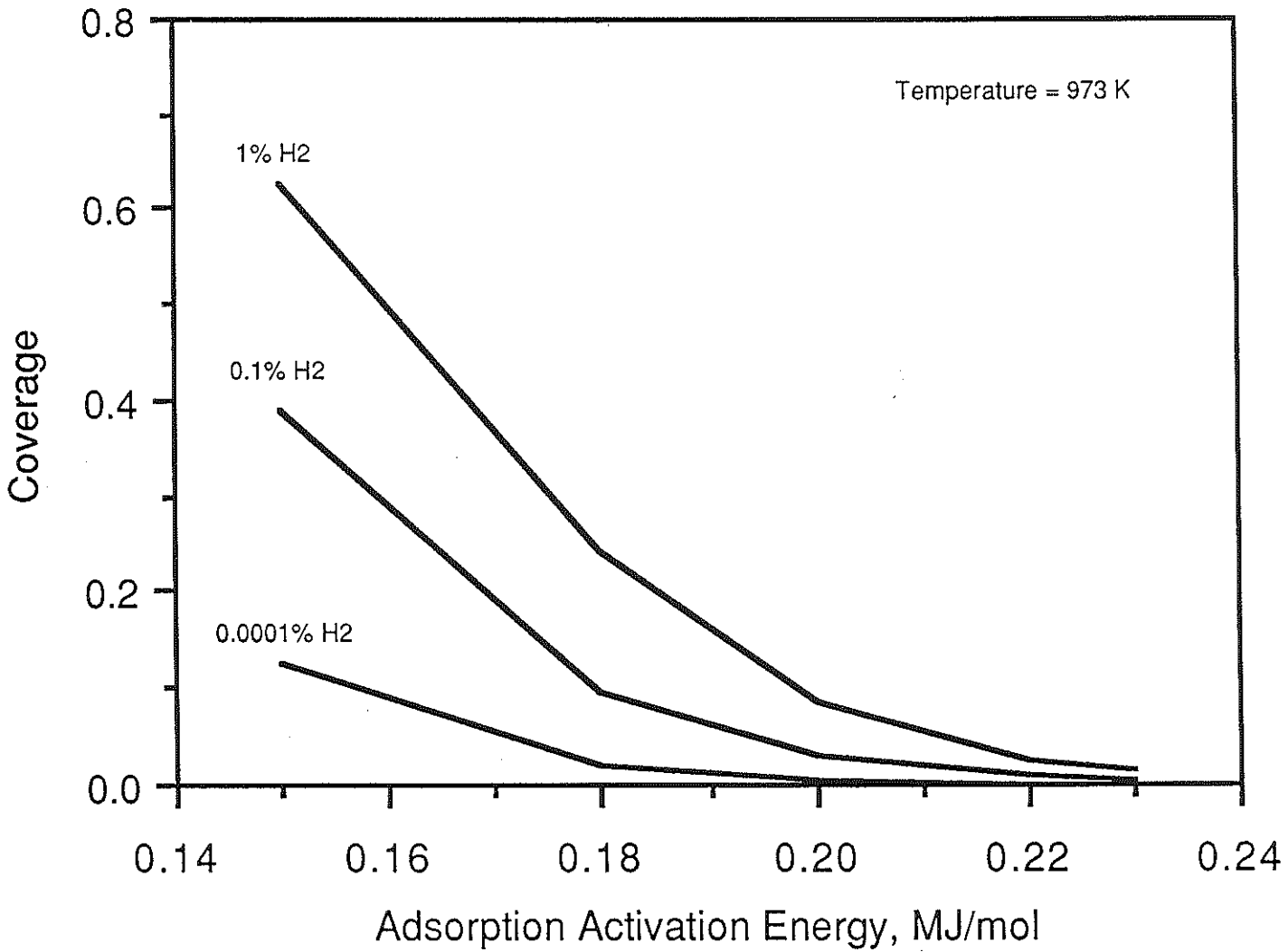
Temperature = 973 K
1% H2
0.1% H2
0.0001% H2
Coverage
0.8
0.6
0.4
0.2
0.0
0.14
0.16
0.18
0.20
0.22
0.24
Adsorption Activation Energy, MJ/mol

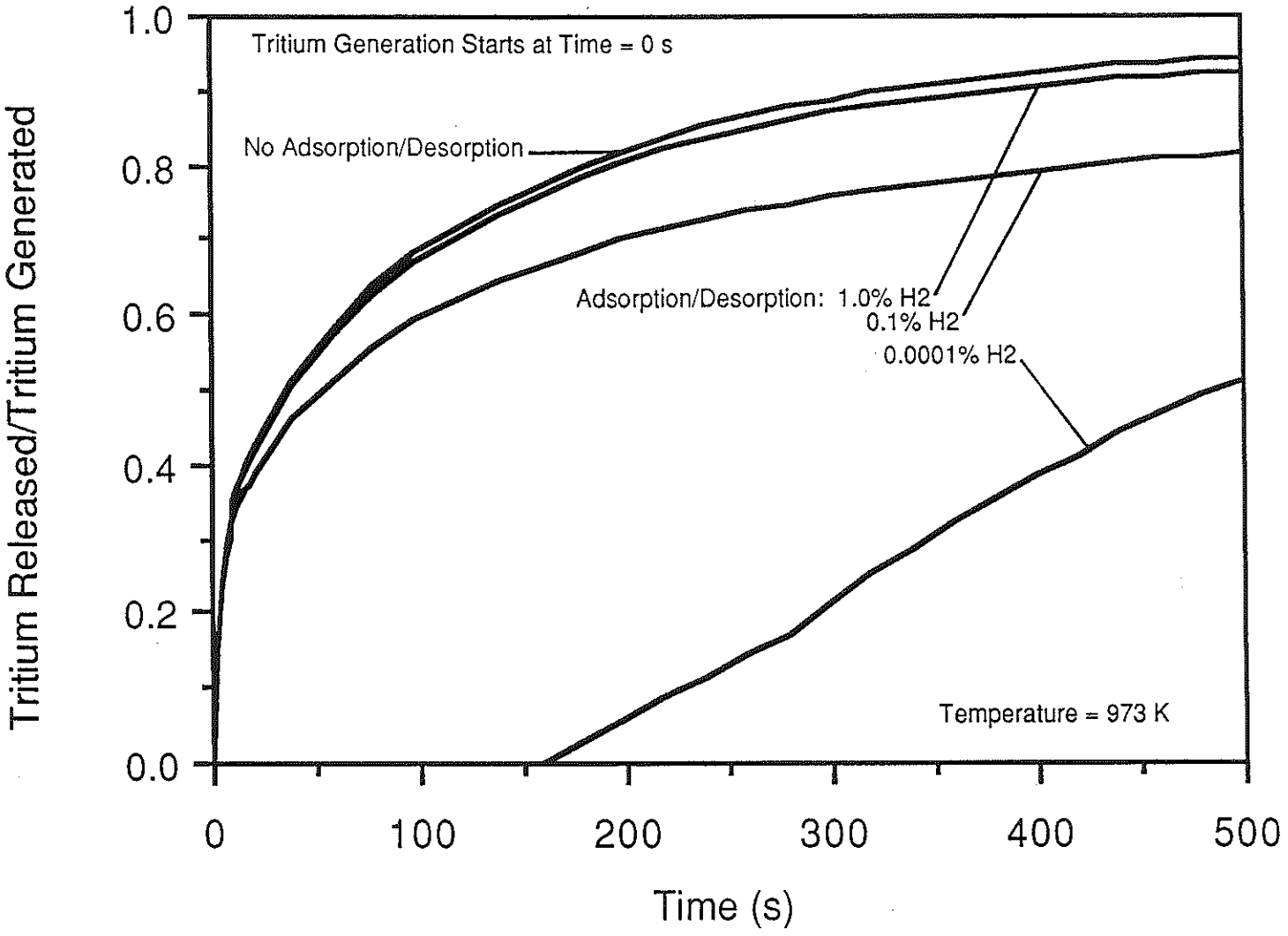
Tritium Generation Starts at Time = 0 s
No Adsorption/Desorption
Adsorption/Desorption: 1.0% H2
0.1% H2
0.0001% H2
Temperature = 973 K
Tritium Released/Tritium Generated
Time (s)
0.0
0.2
0.4
0.6
0.8
1.0
0
100
200
300
400
500

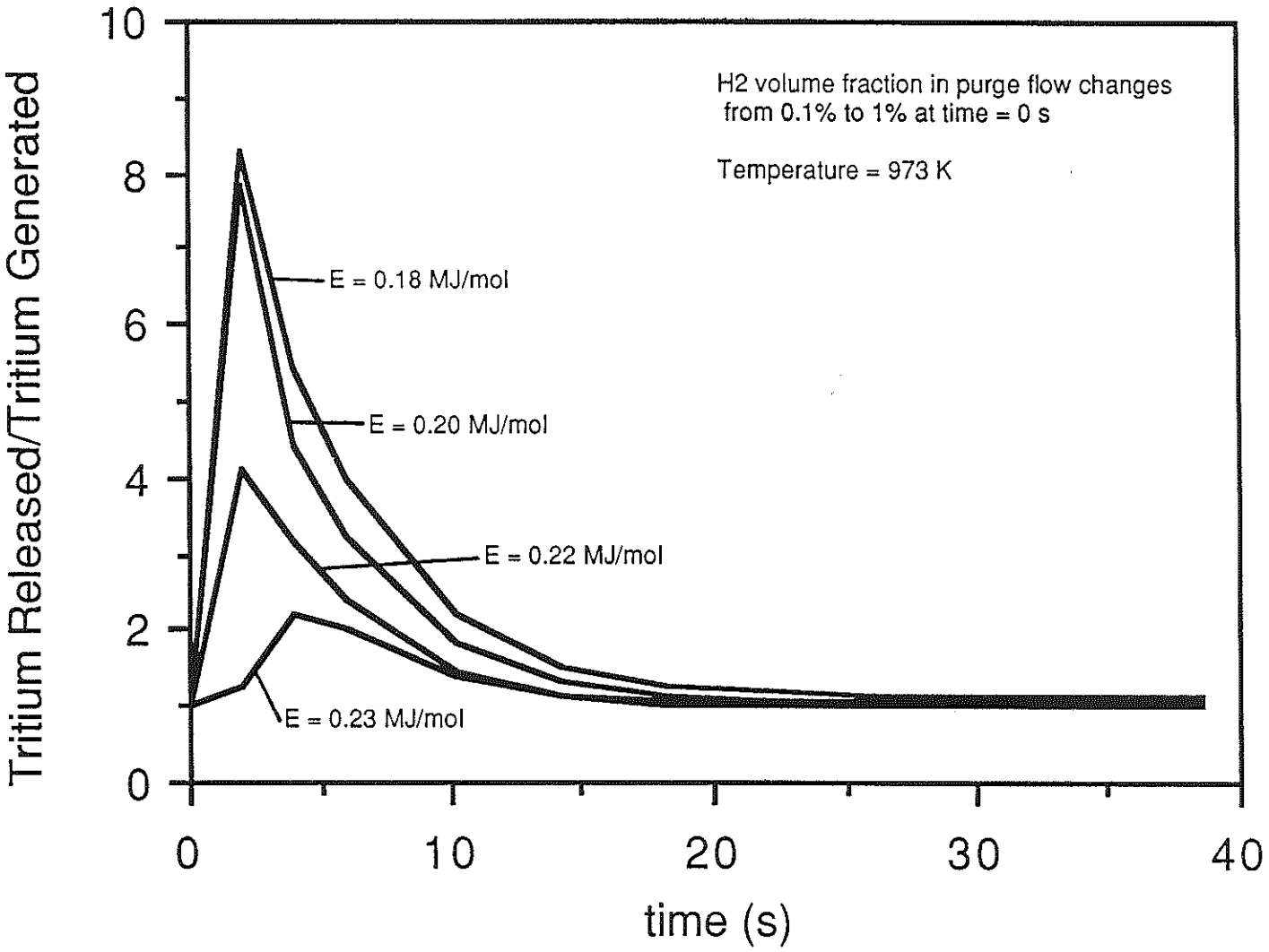
Tritium Released/Tritium Generated
10
8
6
4
2
0
0
10
20
30
40
time (s)
H2 volume fraction in purge flow changes
from 0.1% to 1% at time = 0 s
Temperature = 973 K
E = 0.18 MJ/mol
E = 0.20 MJ/mol
E = 0.22 MJ/mol
E = 0.23 MJ/mol

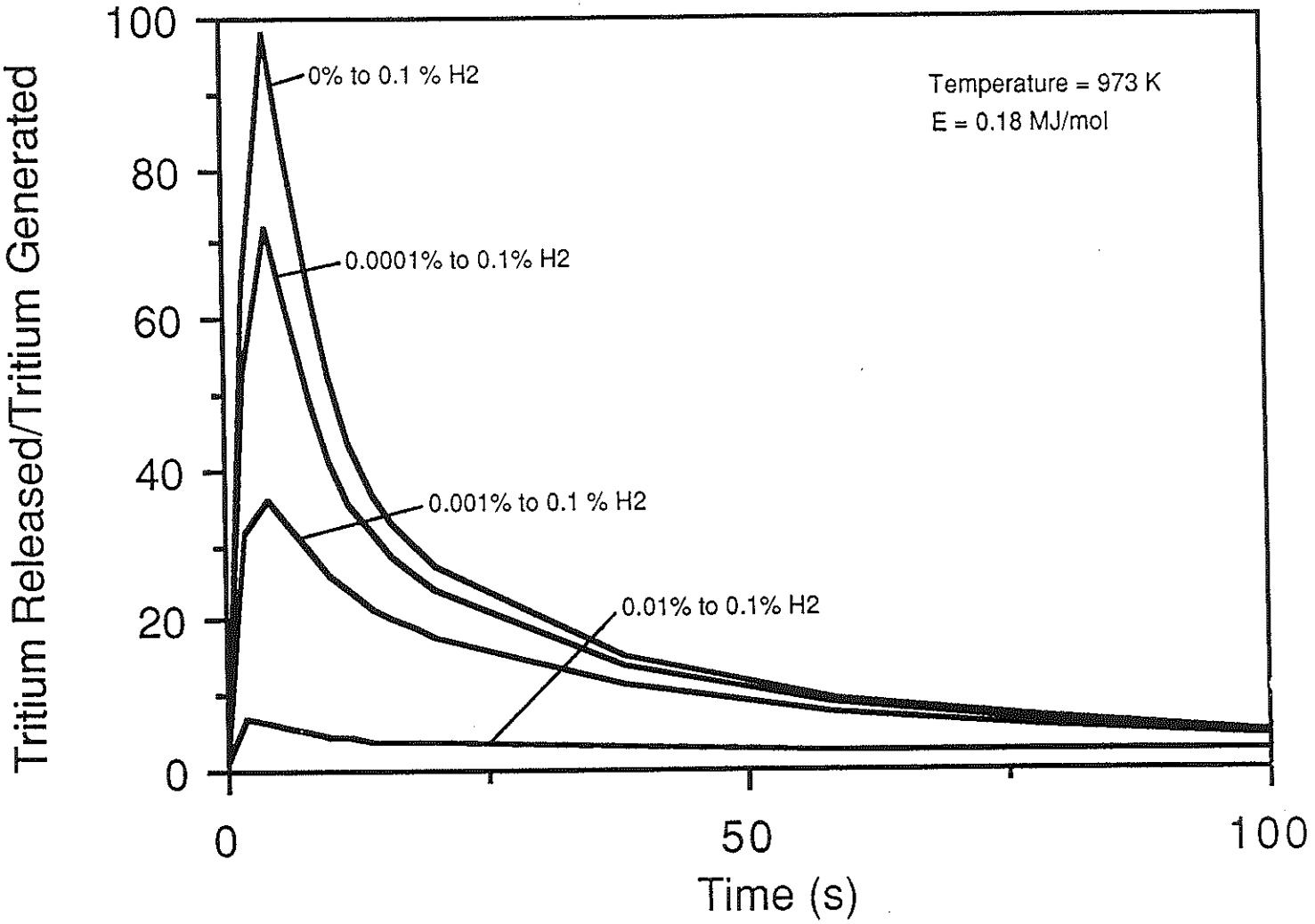
Tritium Released/Tritium Generated
100
80
60
40
20
0
0
50
100
Time (s)
0% to 0.1 % H2
0.0001% to 0.1% H2
0.001% to 0.1 % H2
0.01% to 0.1% H2
Temperature = 973 K
E = 0.18 MJ/mol

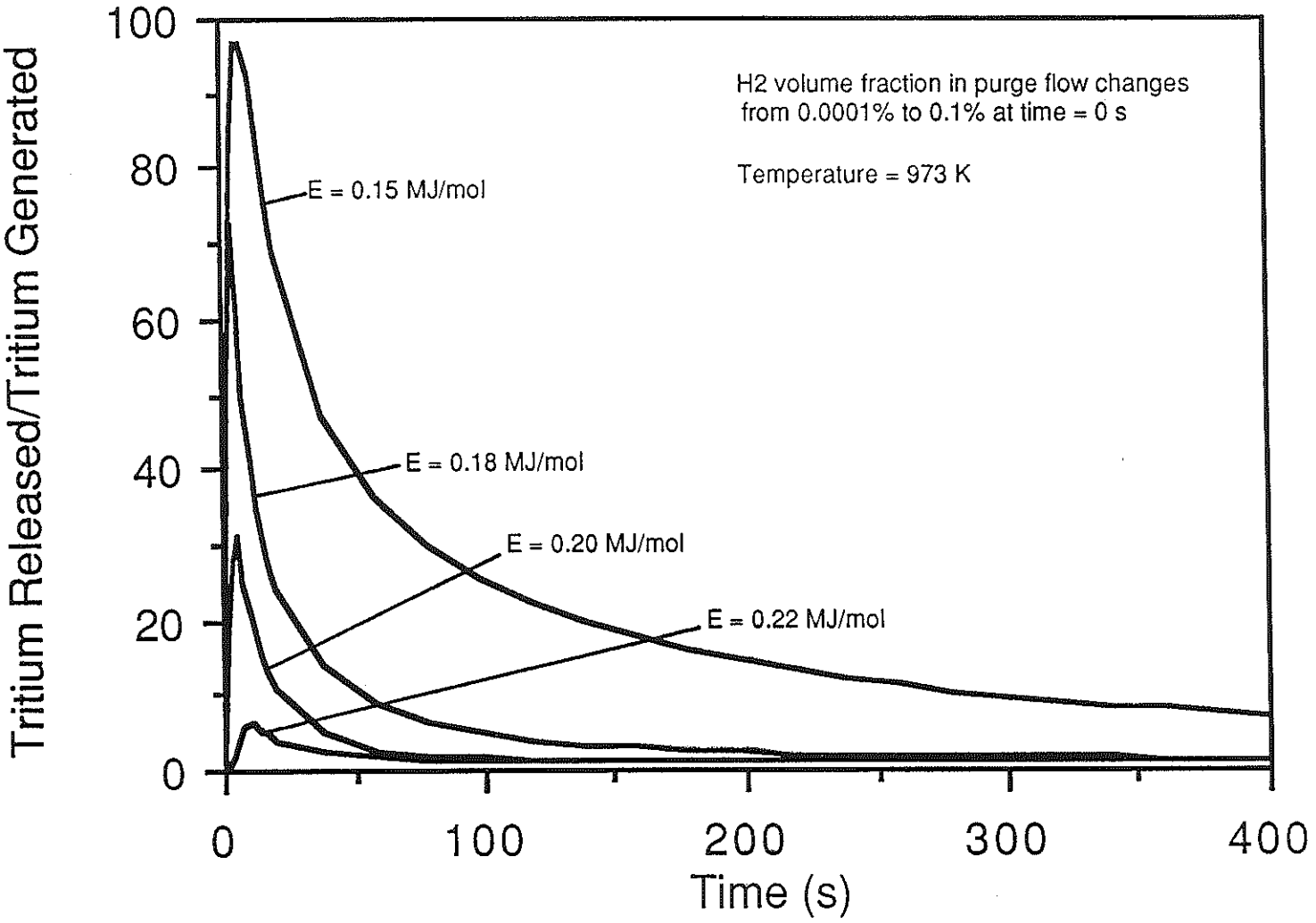
Tritium Released/Tritium Generated
100
80
60
40
20
0
0
100
200
300
400
Time (s)
H2 volume fraction in purge flow changes
from 0.0001% to 0.1% at time = 0 s
Temperature = 973 K
E = 0.15 MJ/mol
E = 0.18 MJ/mol
E = 0.20 MJ/mol
E = 0.22 MJ/mol

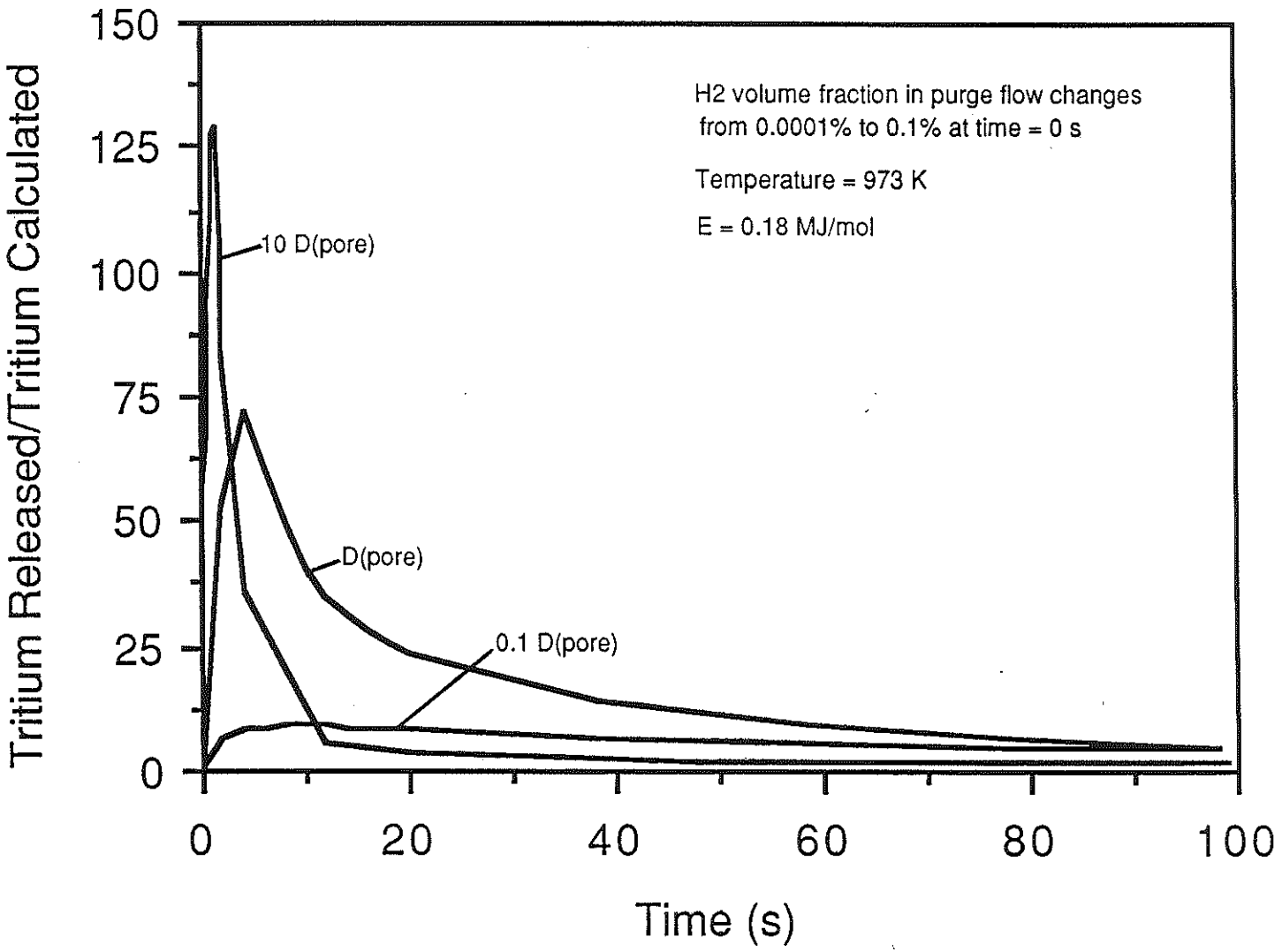
H2 volume fraction in purge flow changes
from 0.0001% to 0.1% at time = 0 s
Temperature = 973 K
E = 0.18 MJ/mol
10 D(pore)
D(pore)
0.1 D(pore)
Tritium Released/Tritium Calculated
Time (s)
150
125
100
75
50
25
0
0
20
40
60
80
100